High-spin states in ^{29}Al and ^{27}Mg

R. Dungan, S. L. Tabor, R. S. Lubna, A. Volya, Vandana Tripathi, B. Abromeit, D. D. Caussyn, K. Kravvaris, and P.-L. Tai

Phys. Rev. C **94**, 064305 — Published 5 December 2016

DOI: 10.1103/PhysRevC.94.064305

High-Spin States in ^{29}Al and ^{27}Mg

R.Dungan, S.L. Tabor, R.S. Lubna, A.Volya, Vandana Tripathi, B.Abromeit, D.D.Caussyn, K.Kravvaris, and P. -L.Tai

Department of Physics,

Florida State University,Tallahassee,FL 32306,USA

Abstract

The structure of ^{29}Al and ^{27}Mg was investigated using the reactions ^{18}O(^{14}C,p2n) and ^{18}O(^{14}C,α n) at 40 MeV. The charged particles were detected and identified with a ΔE-E telescope in coincidence with γ radiation detected in the Florida State University (FSU) Compton suppressed γ detector array. The level and decay schemes of both nuclei have been expanded at higher spins and excitation energies. The positive-parity states up to 3.5 to 4.5 MeV agree well with shell model calculations using the USDA interaction. The negative-parity states in ^{27}Mg are reproduced relatively well by one-particle-hole calculations with the WBP-a interaction. Three ^{27}Mg states unbound by 0.4 to 1.4 MeV to neutron decay were observed to decay radiatively. One of these states had been previously observed to γ decay in a (d,pγ) experiment along with a surprising 16 other neutron unbound states. The competition between neutron and gamma decay in these states is discussed in terms of angular momentum barriers and spectroscopic factors.

I. INTRODUCTION

Nuclei in the *s-d* shell have been investigated experimentally for several decades now. This earlier experimental work used mostly light ion beams which favor lower-spin states and very limited γ detection equipment. The more common availability of heavier beams and larger Compton-supppressed γ detector arrays provides the opportunity to better investigate the higher spin structure of *s-d* nuclei and test newer interactions such as USDA [1, 2] and WBP-a [3]. The more exotic states produced provide an opportunity to further explore the competition between neutron and γ decay above the neutron threshold.

In this work we have used the Florida State University (FSU) long-lived radioactive ^{14}C beam on the heaviest stable Oxygen isotope ^{18}O to populate higher spin states and the FSU particle-Compton-suppressed γ detector array with digital data acquisition to observe their decays in particle-γ-γ coincidence. Particle identification with the ΔE-E telescope allowed very clean separation of the proton and α decay products from each other and from purely neutron decay reaction products. In turn, this allowed a careful comparison of the structure of odd Z (^{29}Al) and odd N (^{27}Mg) nuclei near mid-shell under identical experimental conditions.

Before the present work, no states above 7.2 MeV, no decays above 6 MeV, and no spins above $(11/2^+)$ were known in ^{29}Al. Previous particle transfer studies have used di-neutron transfer on ^{27}Al to measure energies, ℓ transfer values, and spectroscopic factors for ^{29}Al [4–6]. Charged particle angular distributions, level energies, ℓ transfer values, spectroscopic factors, and J^π values had been determined using the pickup reactions ^{30}Si(d,^{3}He) and ^{30}Si(t,α) [7–10]. In-beam γ decay measurements have also been reported in Ref. [5], providing lifetime measurements using the Doppler shift attenuation method (DSAM). Several experiments have observed gamma decays from the ^{26}Mg(α,pγ) reaction to determine excitation energies, branching and mixing ratios, mean lifetimes, γ-ray polarizations, and γ-angular correlations [11–14]. The β-decay of ^{29}Mg produced from the ^{18}O(^{13}C,2p) [15] reaction was used to measure excitation energies and relative β branching intensities in ^{29}Al.

More negative parity states were known in ^{27}Mg, allowing the possibility to further study cross shell excitations. Despite the fact that ^{27}Mg is accessible from single and di-neutron transfer from stable targets [16–18], its higher spin structure was also poorly known. The

gamma decay properties of many states were measured in a ^{26}Mg(d,pγ)^{27}Mg experiment [19]. This paper reports the γ decays of 17 states unbound to neutron decay, a result worthy of further examination. Measurements of γ decays and determination of the neutron separation energy were achieved in a thermal neutron capture on ^{26}Mg experiment [20]. Studies of the β decay of ^{27}Na were achieved from the fragmentation of iridium and uranium targets by protons to measure γ decays, β-γ-γ coincidences, and absolute intensities [21, 22].

II. EXPERIMENT

The ^{18}O(^{14}C,p2n)^{29}Al and ^{18}O(^{14}C,αn)^{27}Mg reactions were studied at the Florida State University (FSU) John Fox Superconducting Accelerator Laboratory to better explore the higher spin structure of these nuclei. A long lived radioactive ^{14}C beam was accelerated to 40 MeV from the FN Tandem before impinging on a Ta_2O_5 target enriched to 97% in ^{18}O of thickness 50 μg/cm^2. A 40μm Tantalum stopping foil separated by 5 mm from the target was used to stop the beam yet allow p,d,t,and α particles to escape with relatively little energy loss. All γ peaks from the reaction were fully Doppler shifted. The target was placed in the target chamber of the FSU Compton suppressed γ array, which for this experiment consisted of three Clover detectors and seven single crystal high purity germanium (HPGe) detectors all surrounded by BGO Compton suppressors. The three Clovers and two single HPGe detectors were placed on a 90° ring. Two of the single HPGe detectors were placed at 35° and the remaining three, at 145°. The HPGe detectors were calibrated for energy and relative efficiency with standard radioactive sources and the 2754 keV line from ^{24}Mg arising from the β decay of ^{24}Na. Additionally, a particle telescope (ΔE-E) was used to detect and identify charged reaction products from the compound nucleus. The telescope consisted of two silicon detectors with the ΔE detector of thickness 0.1 mm and the E detector, of thickness 1.0 mm. The ΔE-E detector was placed behind the target at 0° relative to the beam.

The data acquisition system consisted of a Digital Gamma Finder Pixie16 system [23]. Waveforms from each Ge crystal, each of the BGO photomultiplier tubes, and the E and ΔE Si detectors were sampled at a rate of 100 MHz each. Particle-gamma coincidences and Compton suppression logic as well as pulse energies and arrival times were determined from the waveforms using digital signal processors and field-programmable gate arrays in each

channel of the Pixie16 modules. For this experiment the trigger was set to a minimum of one particle and one gamma.

The data were analyzed using the software GNUSCOPE [24]. Alpha (proton) particle gates were placed on the ΔE-E data to sort α-γ-γ (p-γ-γ) matrices. γ-spectra and γ-γ matrices were corrected for Doppler shifting using an effective recoil velocity β of 0.0280 and 0.0208 for ^{29}Al and ^{27}Mg respectively.

III. RESULTS AND DISCUSSION

A. ^{29}Al

Parts of the spectra of γ rays in coincidence with the 1822, 2276, and new 2989 keV transitions shown in Fig. 1 and 2 provide a view of most of the newly observed lines. The level and decay scheme obtained from the present work is shown in Fig. 3 and tabulated in Table I. All previously reported levels in ^{29}Al were observed in the present experiment up to the $5/2^+$ 3182 keV level.

All the newly discovered states lie above 5900 keV but below the relatively high neutron decay threshold (S_n = 9436 keV). All decay to the $(9/2^+)$ or $(11/2^+)$ levels. The most intense γ decays form a sequence of 5 lines from the highest lying state observed at 8894 keV to the ground state. This is almost certainly an yrast sequence of states because of its preferential population in a reaction which favors high spin states. Indeed, the 3 lowest states were previously known to be yrast. This likely yrast decay sequence is illustrated in the coincidence spectra of Fig. 4. All the coincidences and placement in the level scheme have been verified by reverse gating.

It is informative to compare the level schemes of ^{27}Al and ^{29}Al because both have an unpaired thirteenth proton and even numbers of neutrons. This is shown in Fig. 5. The first 4 states in each have spins of $1/2^+$, $3/2^+$, $5/2^+$, and $7/2^+$, but not in the same order and differences increase at higher energies.

Shell model calculations provide better insight in the structure of ^{27,29}Al. Positive-parity states have been calculated in the shell model using the code COSMO [25] with the USDA

interaction. This interaction [1, 2] was fitted to a considerable amount of structure data for nuclei across the 1s-0d shell and has been very successful. It assumes a closed ^{16}O core and allows unrestricted movement of the remaining nucleons in the 1s-0d shell, but does not consider any excitations into higher shells. These results are also shown in Fig. 5 for ^{29}Al. There is a one-to-one correspondence and very good agreement in energies between theoretical and experimental states up to 4.5 MeV with a Root-Mean-Square (RMS) difference of only 117 keV. When more than one spin assignment was consistent with experiment, we have selected the one suggested by the shell model comparison. This selection is unique up to 4.5 MeV excitation and the excellent agreement makes these assignments almost certain, but such model-dependent assignments are still placed in parentheses in Fig. 5.

Similar USDA shell model calculations for ^{27}Al reproduce its experimental level scheme well with an RMS difference of 101 keV for the states up to 4 MeV. To gain some understanding of why the shell model can predict the differences in structure of these two isotopes, we can look at the expectation values of the occupancies of the 1s-0d orbitals, as shown in Fig. 6. These are shown relative to the naive expectation of all particles occupying the lowest energy orbitals possible: 6 (6) in $\nu d_{5/2}$, 0 (2) in $\nu s_{1/2}$, 5 (5) in $\pi d_{5/2}$ and none in any other orbital for ^{27}Al (^{29}Al). The occupancies differ by 0.3 to 1.8 particle in all the $s-d$ orbitals, showing a significant departure from single-particle structure and essentially equal involvement of protons and neutrons in the structure of these Al nuclei. The strong neutron excitations may explain the lack of similarity of two isotopes differing only in neutron number. Note that the consistent difference in $\nu s_{1/2}$ relative occupancy between the isotopes results partly from the difference of two particles in the reference occupancy. In fact the absolute ground state occupancy for $\nu s_{1/2}$ only changes from 0.6 to 1.2 from ^{27}Al to ^{29}Al while the reference or "expected" number changes from 0 to 2.

Above 4.5 MeV detailed comparisons between experiment and theory for ^{29}Al are not feasible, but the selectivity of the present reaction for yrast and near yrast states and their decay modes allow a closer comparison with theory. As mentioned before, the 5907, 7198, and 8894 keV states in the most strongly populated decay sequence are very likely yrast with spins of $11/2^+$, $13/2^+$, and $15/2^+$, respectively. The 1s-0d shell model does predict good candidates for these at 6300, 6891, and 9099 keV, as well as the other newly observed states, as can be seen in Fig. 7.

B. ^{27}Mg

The ^{27}Mg level and decay scheme obtained from the present experiment is shown in Fig. 8 and listed in Table II. Several α-γ-γ coincidence spectra illustrating the newly observed γ lines in relation to the previously known ones are shown in Figs. 9 and 10. The placement of the new decays in the level scheme was verified by reverse gating.

Over a dozen unbound γ decaying states were reported from a ^{26}Mg(d,pγ) reaction [19] up to E_x = 7976 keV. In the present ^{18}O(^{14}C,αnγ) reaction with different selectivity, we have clearly seen only one of those states at 7858 keV. It agrees in energy with that of Ref. [19] to within 1 keV and in the single decay mode to the very likely $(9/2^+)$ level at 4397 keV. Instead of the other unbound γ decaying states in Ref. [19], two new ones have been produced in the present reaction at 6944 and 7468 keV.

The unpaired neutron in ^{27}Mg is likely a cause of the lower neutron emission threshold making neutron unbound states more experimentally accessible. Here also the newly observed states in ^{27}Mg decay to higher spin states. Levels in ^{27}Mg are compared to those in ^{29}Si which has the same odd number of neutrons (15) in Fig. 11. The first 3 levels follow the same spin sequence but not above this, suggesting that the difference in Z (both even) already affects the structure at relatively low energies.

Also shown in Fig. 11 are the shell model calculations for ^{27}Mg. The USDA [1, 2] interaction constraining all valence particles to the 1s-0d shell was used for the positive parity states. There is very good agreement with experiment with an RMS difference of only 90 keV up through the 3491 keV state. Above this it is likely that some states were not seen experimentally, but there is reasonable agreement among the higher spin states. The spin suggestions shown in parentheses represent the best agreement between theory and experimental energies and decay modes. The relatively higher population of the newly observed 6136 keV state and its decay to $7/2^+$ and $9/2^+$ states suggest an yrast character and spin of $(11/2^+)$ in excellent agreement with the lowest predicted $11/2^+$ state at 6185 keV. The new 7468 keV level is unbound to neutron decay by an MeV and decays only to the 6136 keV $(11/2^+)$ state and not to any lower spin states below. This suggests a higher spin of $(13/2^+)$. The lowest $13/2^+$ state is predicted moderately higher at 7819 keV. Some 2-particle-2-hole (2p2h) admixture in this state might reduce its energy.

Several negative parity states have been reported [26] in ^{27}Mg with spins of $3/2^-$,

$(5/2, 7/2)^-$, $(1/2, 3/2)^-$, and $(5/2^-)$ at 3562, 3762, 4828, and 5373 keV . Comparison with those in ^{29}Si and from shell model calculations provides more insight into the negative parity structure of ^{27}Mg. Theoretical calculations of the negative parity states necessarily involve cross shell excitations by an odd number of nucleons. The WBP-a interaction [3] has been relatively successful for cross shell excitations in nuclei in the upper part of the *s*-*d* shell. This interaction was adapted from the WBP one [27] designed to fit nuclei around A $\approx$ 20 by adjusting the rather undetermined $0f$-$1p$ single particle energies to fit negative parity states in ^{32,34}P. Our calculations have been restricted to one hole (particle) in the $0p$ ($0f$-$1p$) shell which should represent well the lowest negative parity states. Of the two possible spins for the 3762 keV level, $7/2^-$ is more likely because of the corresponding 3623 keV $7/2^-$ state in ^{29}Si and and the 3384 keV state predicted in the shell model. The calculations suggest a choice of $1/2^-$ for the experimental 4828 keV state because of its proximity to the predicted $1/2^-$ level at 5007 keV. The fact that the calculated expection values of occupancy for the 4204 keV $1/2^-$ and 5381 keV $3/2^-$ states indicate that they are predominantly (70% - 75%) $0p$ hole states would explain why they haven't been seen in (d,p) reactions which favor states with a neutron added to the ^{26}Mg ground state. In turn the observed 4828 $\rightarrow$ 3491 keV decay [19] rules out $5/2^+$ for the lower state, leaving the alternative $3/2^+$ assignment which agrees with the USDA shell model calculation. The 5829 keV level in ^{27}Mg decays to the $(7/2^-)$ and $(9/2^+)$ states. Decay to a negative parity state and the fact that no ℓ value has been reported for the neutron transfer to this level suggest negative parity and moderately high spin and a likely correspondence to the $7/2^-$ states at 6193 keV in ^{29}Si and 5666 keV in the WBP-a calculations, although $11/2^-$ is also a good possibility due to the 5317 keV theoretical state. The $11/2^-$ states at 6781 keV in ^{29}Si and 6763 keV in theory suggest $11/2^-$ for the 6944 keV state in ^{27}Mg, as does the γ (as opposed to neutron) decay of this unbound level.

The WBP-a interaction, originally adjusted to fit heavier nuclei, does a relatively good job reproducing the negative parity one-particle-one-hole states in mid-shell ^{27}Mg. The RMS deviation for the 6 experimental states compared to theory of 233 keV is good for cross shell excitations but more than twice that for the pure *s*-*d* states. This value uses $7/2^-$ for the 5829 keV experimental states which agrees better with what is known in ^{29}Si and the WBP-a energy. However a question remains as to why the lowest predicted $11/2^-$ level at 5317 keV was not seen in an experiment which generally favors yrast states.

A rather surprising observation mentioned earlier is that 17 unbound states were observed to decay by γ emission in a (d,pγ) experiment [19]. One of these states was seen in the present work, as well as two previously unreported γ decaying unbound states. So many radiatively decaying states, especially produced in a (d,p) reaction which favors lower spin states, might not be expected since the generally much stronger neutron decay can only be inhibited by the angular momentum barrier and small neutron decay spectroscopic factors. The angular mementum barrier is estimated in Table III based on the decay neutron energy and the highest spin the parent state could have, limited by its known γ decays assuming they are M1 transitions. A check of shell model predictions shows that the distribution of assumed spins in Table III is very close to what the shell model predicts. The estimated Γ_n values were calculated with a simple square well penetrability program called `nucracker` [25] following the Bohr and Mottleson prescription [28] and assume unit spectroscopic factors.

To give a rough electromagnetic decay scale, a 1 Weisskopf unit M1 transition of 2 MeV would have a decay width of 0.16 eV. More than half of the neutron penetrability estimates exceed this value. This does not have to conflict with the observation of γ decay because neutron decay spectroscopic factors much less than unity will further reduce their widths. Spectroscopic factors below 10^{-4} were inferred in the γ decay of unbound states in ^{19}O [29] and ^{21}O [30]. While such very low spectroscopic factors can explain the predominance of radiative over neutron decay, they lead to another question: how could these states have been populated with observable strength in the (d,p) neutron transfer reaction?

More information on unbound states comes from a neutron resonance experiment on ^{26}Mg which measured both neutron and γ decays [31] of low spin unbound states. Results relevant to the present work are listed in Table IV. Neutron and γ decays were observed with Γ_γ/Γ_N ratios ranging from 10^{-4} to 10^{-2}. The γ decay strengths are generally larger than expected for the higher spin states because multiple decays whose energies would be much higher are possible to the lowest states. The neutron decay widths, while much larger than those for radiative decays, are lower than the angular momentum barrier penetrabilities. This ratio, the spectroscopic factor S, spans a wide range from 2.7×10^{-5} to 0.39, a range consistent with the values needed to permit γ decay of the higher spin states discussed above.

IV. SUMMARY

The ^{29}Al and ^{27}Mg nuclei were studied using the ^{18}O(^{14}C,p2nγ)^{29}Al and ^{18}O(^{14}C,αnγ)^{27}Mg reactions, respectively, with the FSU particle-γ detector array. The level and decay schemes were extended significantly by careful examination of the p-γ-γ and α-γ-γ matrices. This reaction brings in more angular momentum than most previous ones and preferentially populates the highest spin states available in the energy regions. The newly observed states generally decay into the previously known levels of highest spin.

New levels up to almost 9 MeV in excitation energy in ^{29}Al with relatively high spins were identified. A total of 8 new states (with one marked tentative) and 11 new γ transitions were observed. Three of these new γ transitions extend the previously known highest spin decay sequence, suggesting an yrast sequence of M1 transitions from $(15/2^+)$ down to $5/2^+$. The shell model using the USDA interaction in the 1s-0d shell reproduces well the states up to 4.5 MeV excitation and provides good candidates for the newly observed states.

A total of 4 new states and 6 new γ transitions were identified in ^{27}Mg. Comparison with ^{29}Si and shell model calculations have improved the picture of the negative-parity states with the suggested assignments of $7/2^-$ to the 5829 keV state and $11/2^-$ to the newly observed 6944 keV level. There is excellent agreement in energy up to 3.5 MeV between the experimental positive-parity states with the predictions of the 1p-0d shell model using the USDA interaction. Calculations with the WBP-a interaction allowing exactly one additional nucleon to move into or out of the 1s-0d shell reproduce the observed negative-parity states relatively well, especially considering the higher excitation energies involved (3.5 - 7 MeV). A consequence of the mid-shell position of ^{27}Mg with only 4 protons in the s-d shell and a neutron number only 5 below shell closure is that cross shell excitations of $0p \rightarrow s$-d and s-$d \rightarrow 0f$-$1p$ compete at comparable energies.

A review of the literature on ^{27}Mg revealed a surprising result of 17 γ decaying neutron unbound states seen in a old (d,pγ) experiment which had not been discussed. The observation of one of these states in the present experiment with the same decay mode provides some confirmation of the earlier result. Our estimates of the spins of those states and their neutron penetrabilities show that radiative decay could not compete with neutron decay for many of them unless neutron decay were further surpressed by very small spectroscopic factors, as was seen for ^{19,21}O. The low spectroscopic factors implied by the observation of

dominant radiative decays for these higher spin states are in the same range as those directly measured by a neutron resonance experiment for low spin unbound states. These results along with those from ^{19,21}O show that γ decay from moderately unbound states should not be underestimated.

ACKNOWLEDGMENTS

This work was supported in part by U.S. National Science Foundation under grant NSF 14-01574 and in part by the U.S. Department of Energy Office of Science, Office of Nuclear Physics under Grant No. DE-SC0009883.

[1] W. A. Richter, S. Mkhize, and B. Brown, Phys. Rev. C., **78**, 064302 (2008).

[2] B. Brown and W. Richter, Phys. Rev. C., **74**, 034315 (2006).

[3] P. Bender *et al.*, Phys. Rev. C, **80**, 014302 (2009).

[4] A. A. Jaffe *et al.*, Proceedings of the Physical Society, **76**, 6 (1960).

[5] A. D. W. Jones, J. A. . Becker, and R. E. McDonald, Phys. Rev. C, **3**, 724 (1971).

[6] L. C. Bland *et al.*, Nuclear Physics A., **431**, 237 (1984).

[7] R. C. Bearse, D. H. Youngblood, and J. L. Yntema, Phys.Rev., **167**, 1043 (1968).

[8] A. D. W. Jones, Phys. Rev., **180**, 997 (1969).

[9] H. Mackh, G. Mairle, and G. J. Wagner, Z.Phys., **269**, 353 (1974).

[10] J. S. Hanspal *et al.*, Nucl. Phys. A, **455**, 494 (1986).

[11] F. A. Beck, T. Byrski, G. Costa, and P. Engelstein, Nucl. Phys. A, **218**, 213 (1974).

[12] P. Ekström and J. Tilman, Nucl. Phys. A, **230**, 285 (1974).

[13] J. R. Williams, R. O. Nelson, C. R. Gould, and D. R. Tilley, Phys. Rev. C, **11**, 1111 (1975).

[14] F. A. Beck, T. Byrski, A. Knipper, and J. P. Vivien, Phys. Rev. C, **13**, 1792 (1976).

[15] D. R. Goosman, C. N. Davids, and D. E. Alburger, Phys. Rev. C, **8**, 1331 (1973).

[16] S. Hinds, H. Marchant, and R. Middleton, Proc. Phys. Soc., **78**, 473 (1961).

[17] R. N. Glower, Physics Letters, **16**, 147 (1965).

[18] F. Meurders and A. Van Der Steld, Nucl. Phys. A, **230**, 317 (1974).

[19] W. Brendler, P. Betz, E. Bitterwolf, and H. Ropke, Z.Phys. A, **281**, 75 (1977).

[20] T. A. Walkiewicz *et al.*, Phys. Rev. C, **45**, 1597 (1992).

[21] C. Détraz *et al.*, Phys. Rev. C, **19**, 164 (1979).

[22] D. Guillemaud-Mueller *et al.*, Nucl. Phys. A, **426**, 37 (1984).

[23] "XIA LLC," `http://www.xia.com/DGF_Pixie16.html/` (2016).

[24] J.Pavan, Ph.d dissertation (2004).

[25] A.Volya, `http://www.volya.net` (2015).

[26] ENSDF, "NNDC Online Data Service, ENSDF database," `http://www.nndc.bnl.gov/ensdf/` (2015).

[27] E. Warburton and B. Brown, Phys. Rev. C, **46** (1992).

[28] A. Bohr and B. R. Mottleson, *Nuclear Structure*, Vol. I (W. A. Benjamin, Inc., 1969) Chap. 3F.

[29] R. Dungan *et al.*, Phys. Rev. C, **93**, 021302(R)1 (2016).

[30] M. Stanoiu *et al.*, Phys. Rev. C, **69**, 034312 (2004).

[31] C. Massimi *et al.*, Phys. Rev. C, **85**, 044615 (2012).

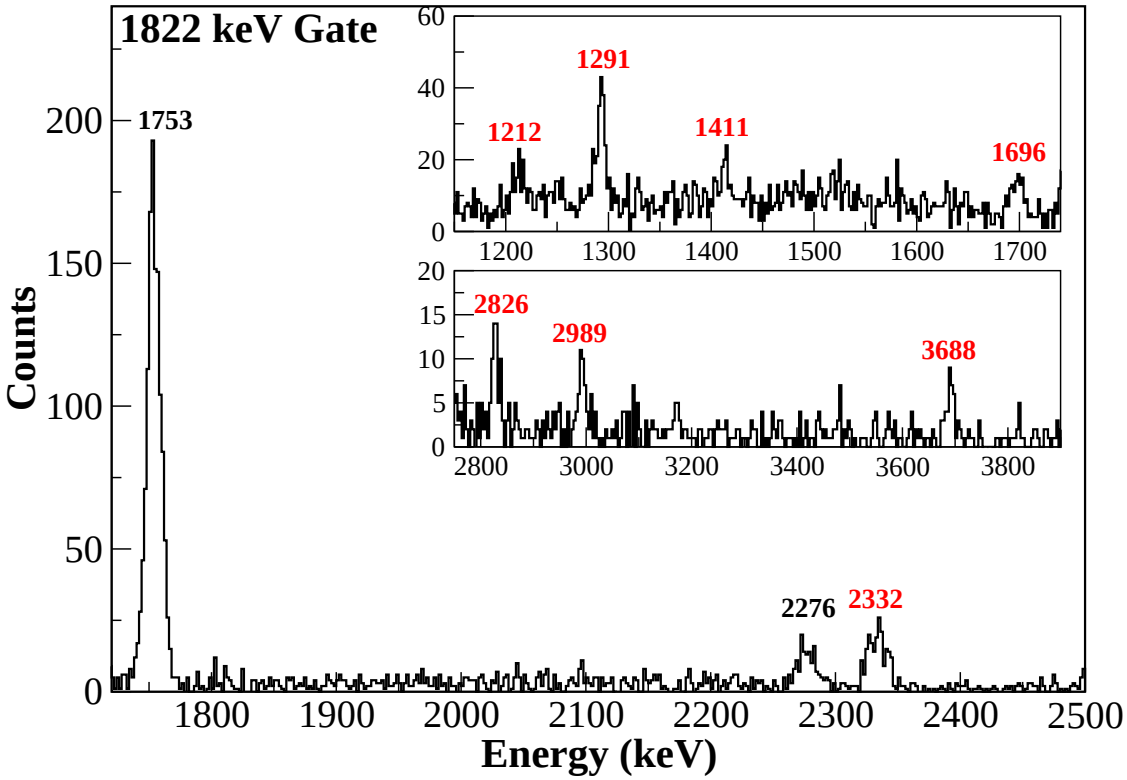

FIG. 1: Three different regions of the γ-ray energy spectrum in coincidence with protons and the 1822 keV γ ray from ^{29}Al. Labeled in black (red) are previously (newly) observed γ lines in ^{29}Al.

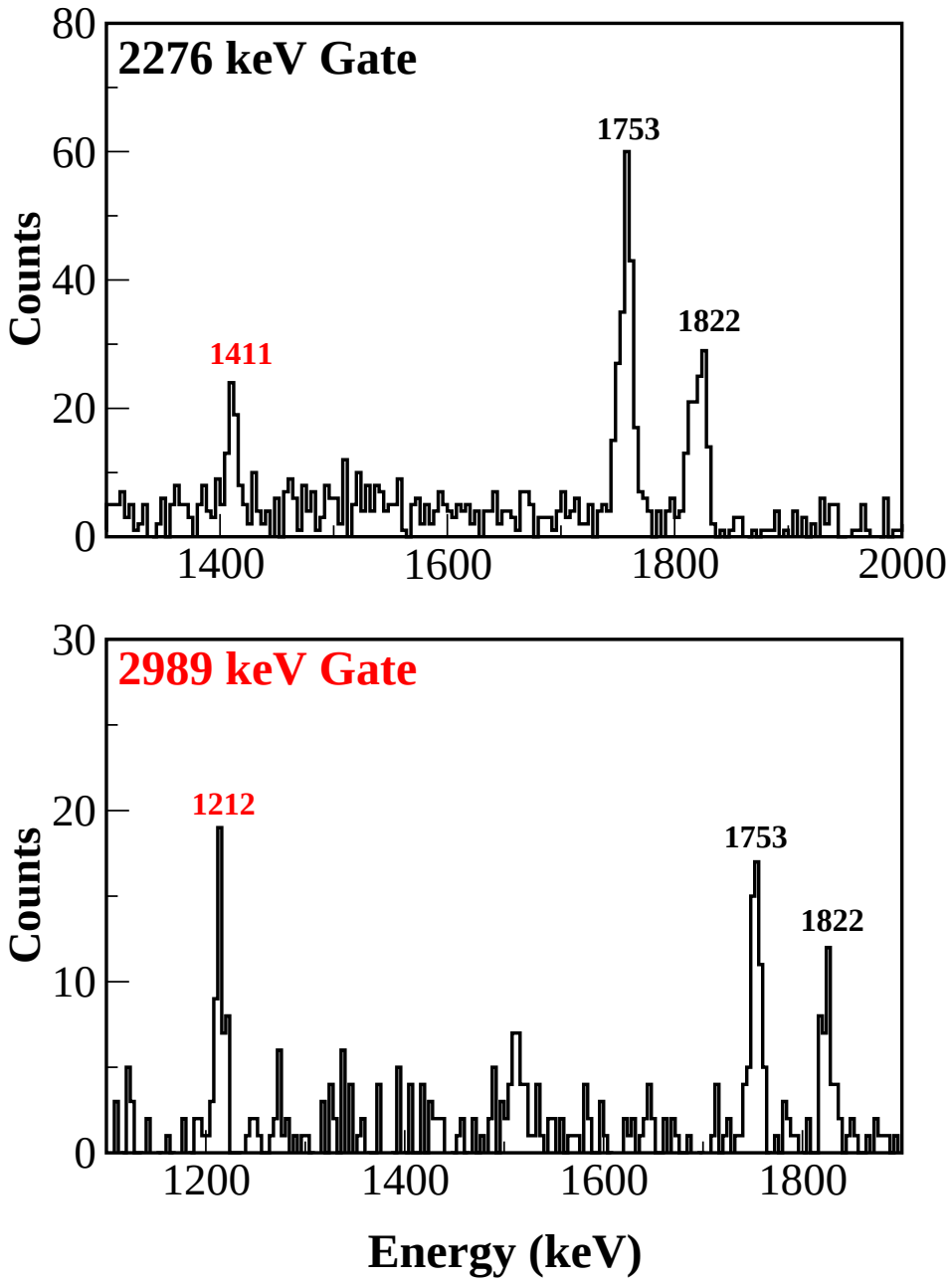

FIG. 2: Two spectra showing the γ spectra in coincidence with the 2276 keV (top) and the 2989 keV (bottom) γ lines from ^{29}Al. Newly observed states and transitions are shown in red.

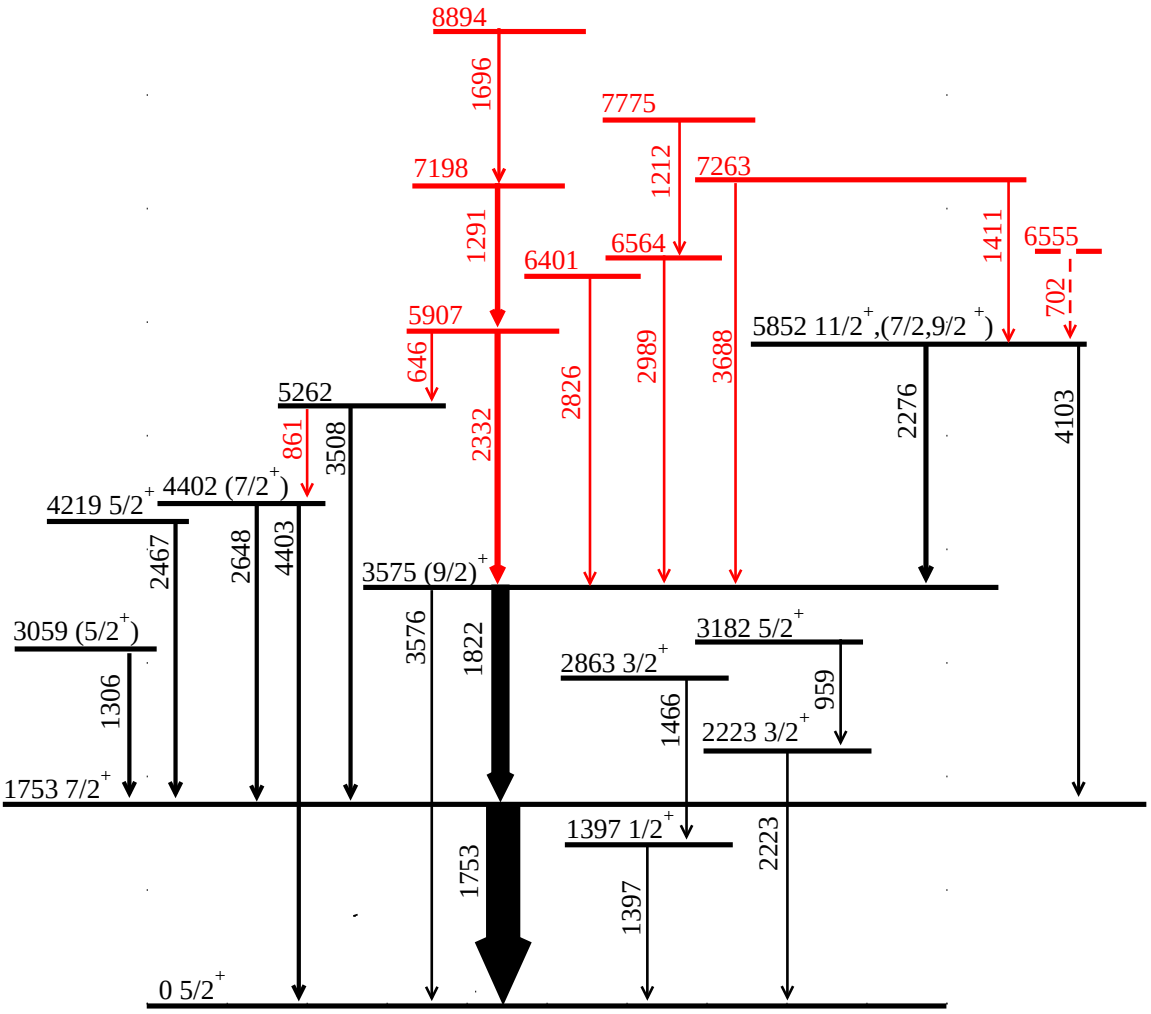

FIG. 3: Energy level and decay scheme of ^{29}Al obtained from the present work. States and decay lines which were previously reported (newly observed in this work) are shown in black (red). The widths of the arrows indicate the γ intensities relative to that of the 1753 keV line.

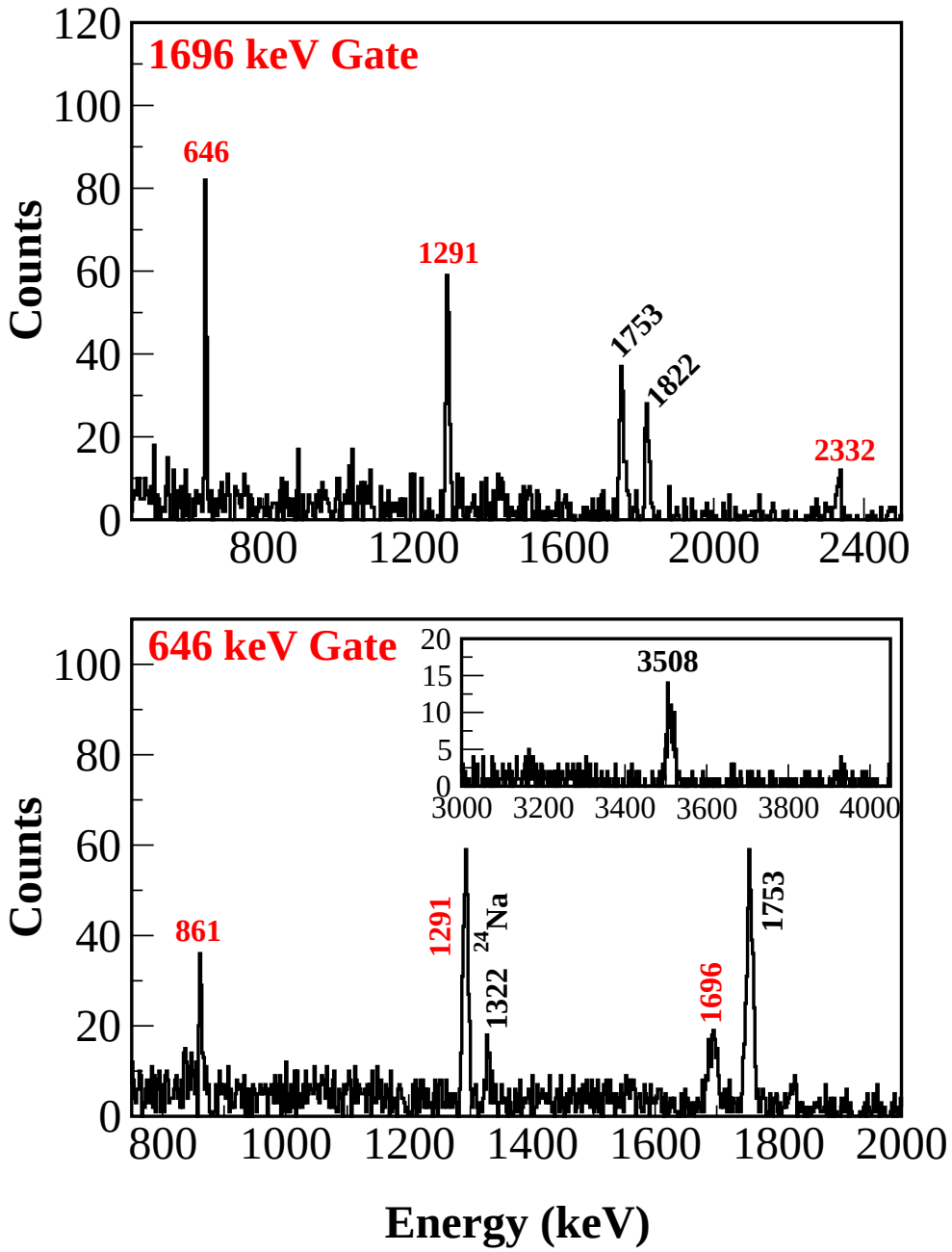

FIG. 4: A portion of the γ-ray energy spectrum in coincidence with protons and the 1696 or 646 keV γ rays from ^{29}Al. Labeled in black (red) are previously (newly) observed γ lines

TABLE I: Excitation energies, γ transitions, and relative intensities I_γ observed in ^{29}Al from the present experiment.

E_x(keV)	E_γ (keV)	$2J_i^\pi$ ($\hbar$)	$2J_f^\pi$ ($\hbar$)	I_γ(%)
1397 (1)	1397 (1)	1^+	5^+	2.1 (5)
1752.9 (4)	1752.9 (4)	7^+	5^+	100
2223 (2)	2223 (2)	3^+	5^+	6 (3)
2863 (3)	1466 (3)	3^+	1^+	< 2
3059 (3)	1306 (3)	(5^+)	7^+	3.0 (8)
3182 (2)	959.2 (5)	5^-	3^+	4.0 (5)
3575 (2)	1822 (1)	(9^+)	7^+	58 (7)
	3576 (3)	(9^+)	5^+	7 (2)
4219 (3)	2467 (3)	5^+	7^+	5 (1)
4402 (3)	4403 (3)	(7^+)	5^+	7 (2)
	2648 (2)	(7^+)	7^+	2.1 (6)
5262 (3)	3508 (3)		7^+	8 (2)
	861 (2)		(7^+)	1.8 (5)
5852 (3)	2276 (2)	11^+,$(7,9^+)$	(9^+)	11 (2)
	4103 (4)	11^+,$(7,9^+)$	7^+	7 (3)
5907 (3)	2332 (2)		(9^+)	20 (4)
	645.9 (5)			11 (2)
6401 (4)	2826 (3)		(9^+)	4 (1)
6555 (3)	702 (1)		11^+,$(7,9^+)$	2.7 (6)
6564 (4)	2989 (3)		(9^+)	4 (1)
7198 (3)	1291 (1)			16 (3)
7263 (4)	3688 (4)		(9^+)	4 (1)
	1411 (3)		11^+,$(7,9^+)$	4 (1)
7775 (5)	1212 (3)			2.4 (6)
8894 (4)	1696 (3)			5 (1)

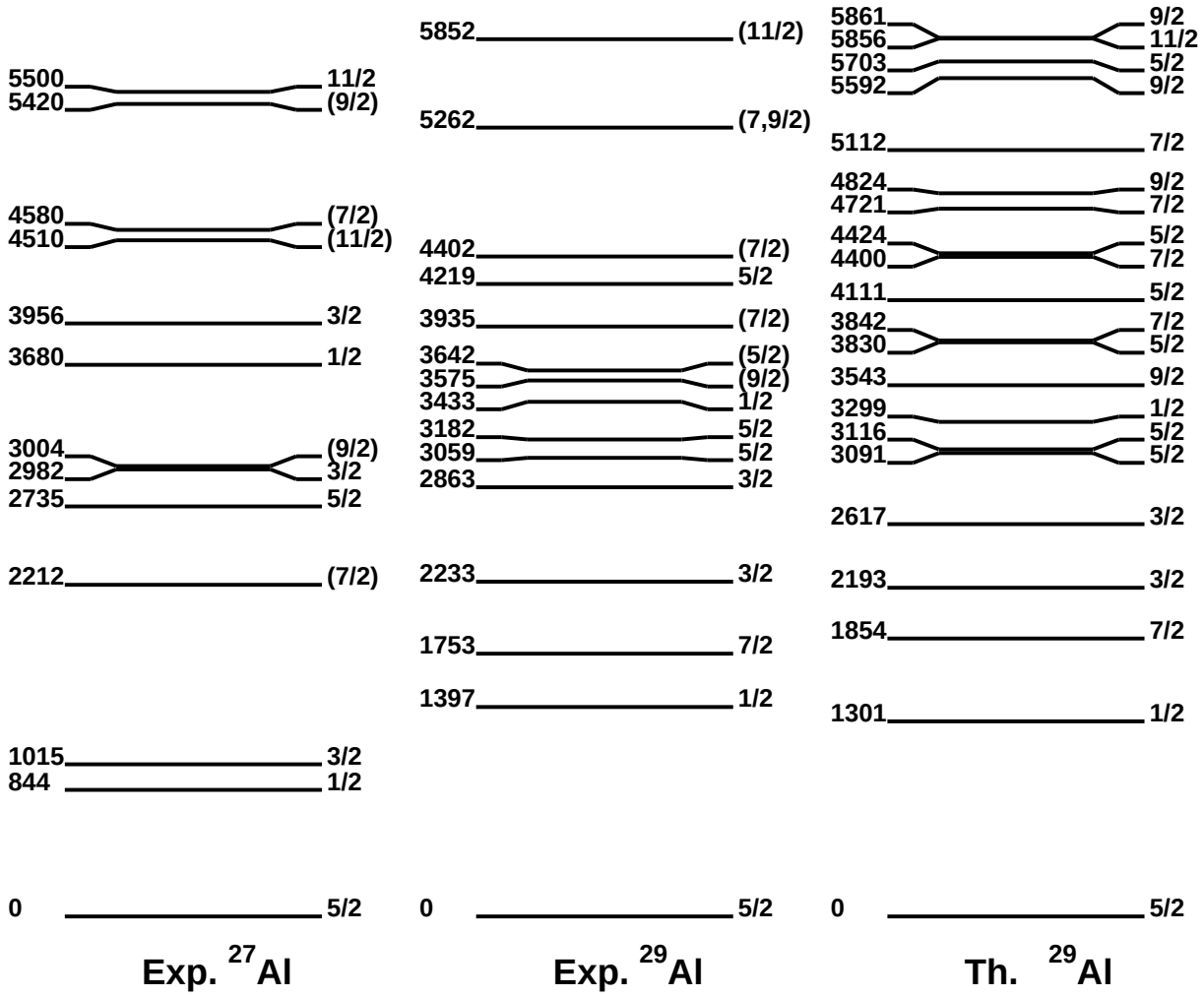

FIG. 5: A comparison of positive-parity excited states in ^{27,29}Al up to 5900 keV and shell model calculations for ^{29}Al using the USDA interaction in the 1s-0d shell. Only states of spin $5/2^+$ and higher are shown above 4500 keV. Note that some previously reported states not observed in the present experiment are included for completeness. All parities are positive.

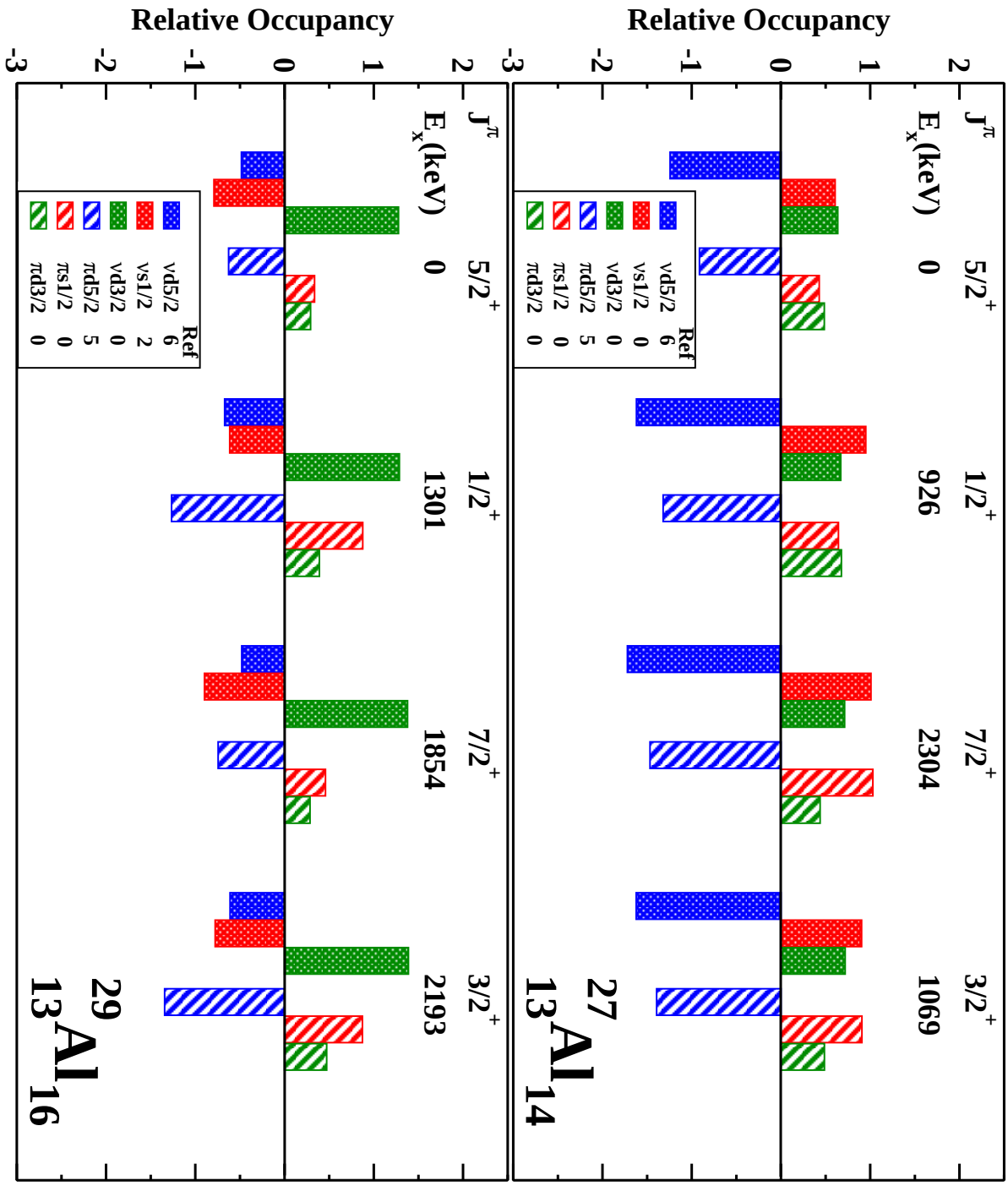

FIG. 6: Relative occupancies of the $1s$-$0d$ orbitals for the lowest four states in ^{27,29}Al calculated in the shell model using the USDA interaction. The occupancies are shown relative to the expectations of the extreme single particle model whose values are shown under the label "Ref". Note that the reference for ^{29}Al contains 2 neutrons in the $s_{1/2}$ orbital which are not in the ^{27}Al reference, leading to the large differences in the figure for $s_{1/2}$ occupancies between these two isotopes, as discussed in the text.

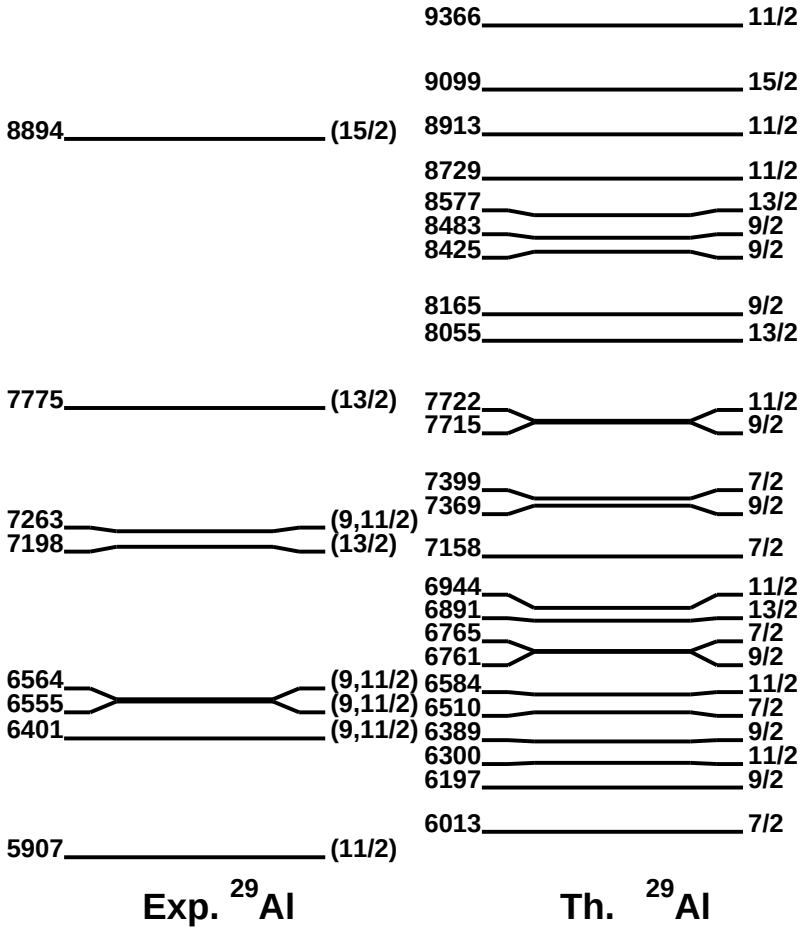

FIG. 7: The newly observed positive parity states in ^{29}Al above 5900 keV are compared with USDA shell model predictions. Only states of spin $\geq 7/2^+$ are shown among the USDA calculations. Above 7500 keV only states of spin $\geq 9/2^+$ are represented.

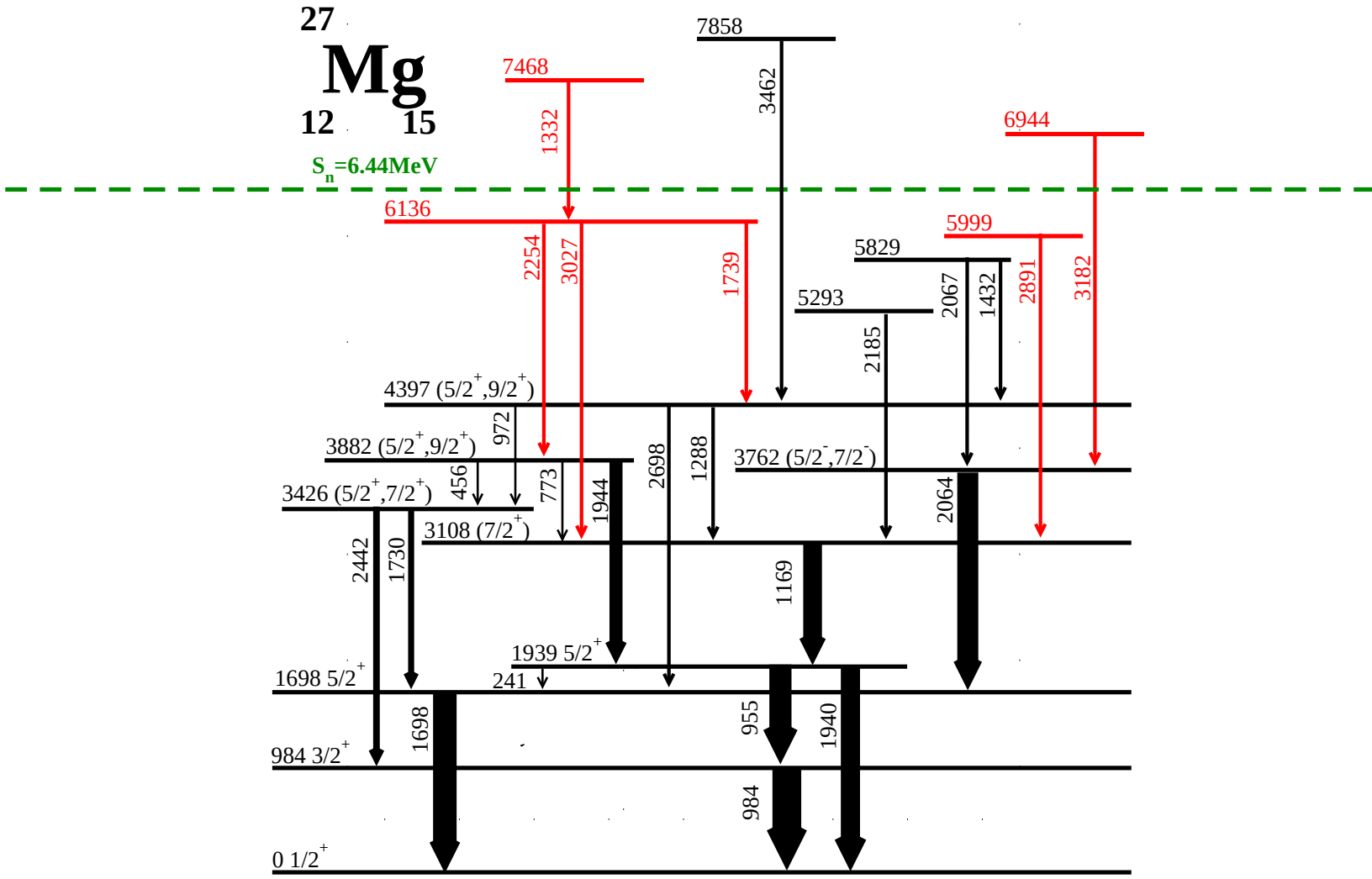

FIG. 8: Energy level and decay scheme of ^{27}Mg obtained from the present work. Shown are states and γ lines (in keV) that have been previously identified (black) and newly observed (red). The widths of the arrows indicate the γ intensities relative to that of the 984 keV line.

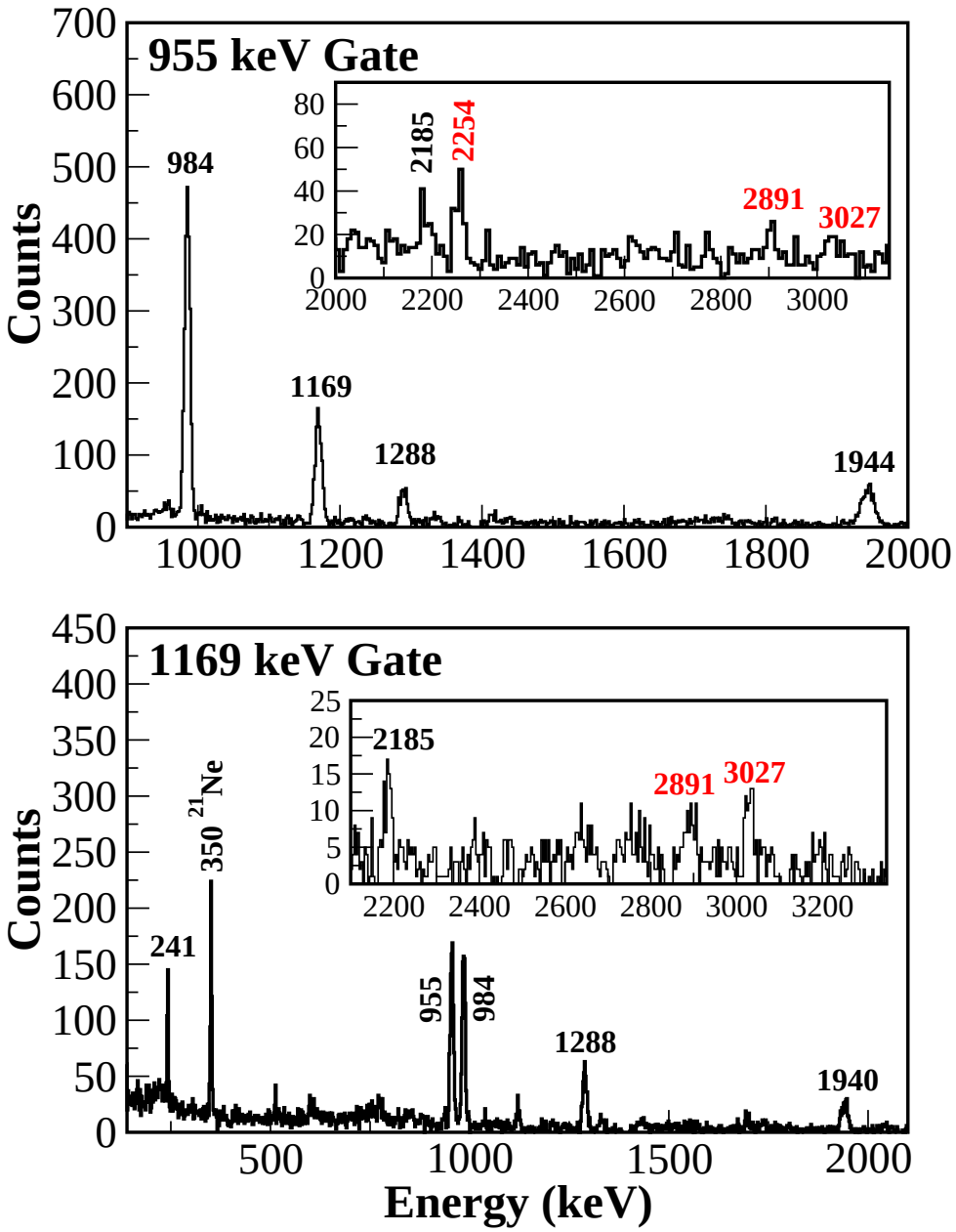

FIG. 9: Two spectra showing the γ spectra in coincidence with the 955 keV (top) and the 1169 keV (bottom) γ lines from ^{27}Mg. Newly observed states and transitions are shown in red.

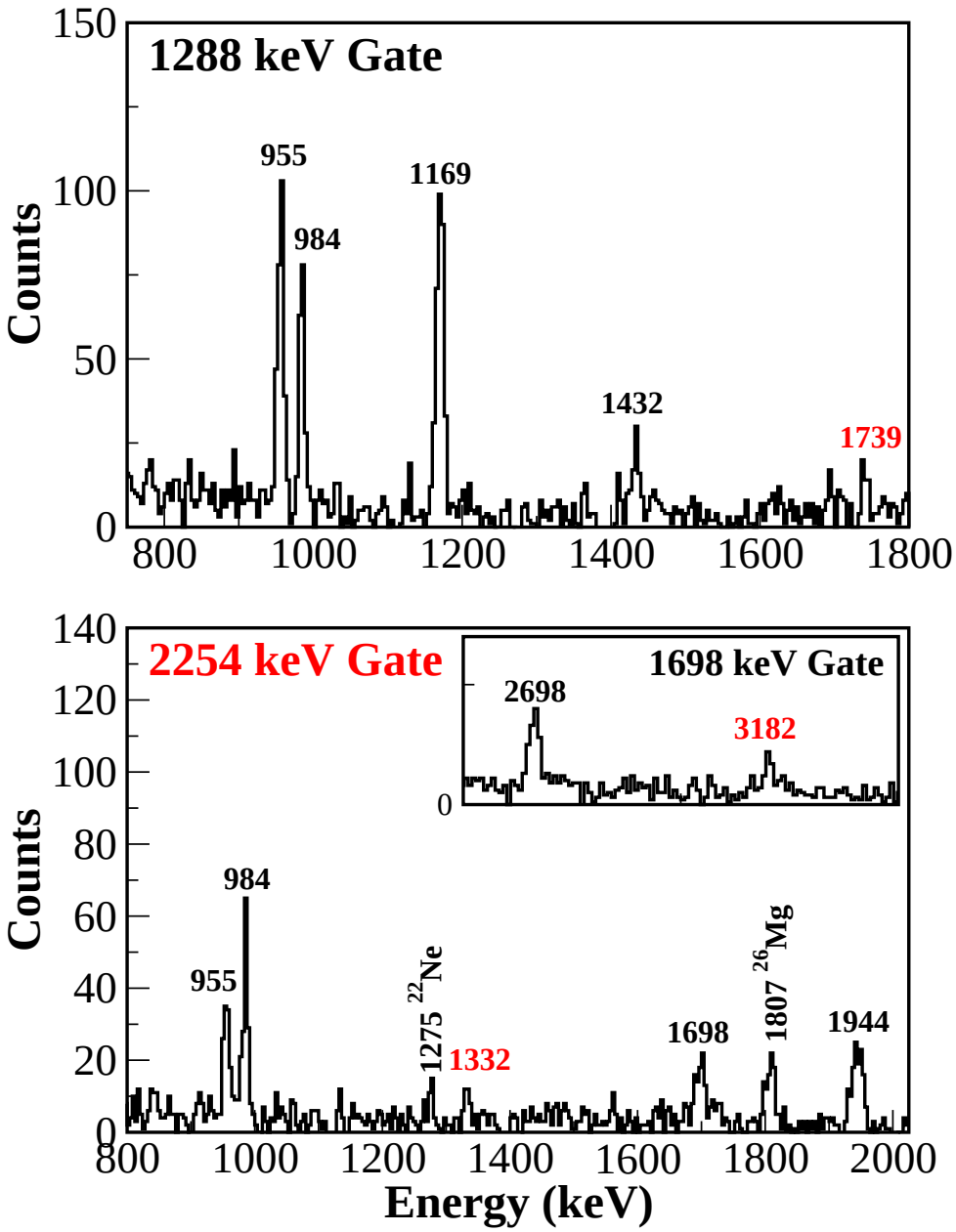

FIG. 10: Portions of the γ spectra in coincidence with the 1288, 2254, and 1698 (inset) keV γ-rays from ^{27}Mg. Labeled in black (red) are previously (newly) observed γ lines in ^{27}Mg.

TABLE II: Excitation energies, γ transitions, and relative intensities I_γ observed in ^{27}Mg from the present experiment.

E_x(keV)	E_γ (keV)	$2J_i^\pi$ ($\hbar$)	$2J_f^\pi$ ($\hbar$)	I_γ(%)
984 (1)	984 (1)	3^+	1^+	100
1698 (1)	1698 (1)	5^+	1^+	78 (8)
1939 (1)	955 (1)	5^+	3^+	78 (8)
	241.1 (5)	5^+	5^+	8 (2)
	1940 (1)	5^+	1^+	38 (7)
3108 (2)	1169 (1)	(7^+)	5^+	56 (6)
3426 (2)	2442 (1)	$(5^+,7^+)$	3^+	29 (5)
	1730 (2)	$(5^+,7^+)$	5^+	20 (3)
3762 (2)	2064 (2)	$(5,^-,7^-)$	5^+	
3882 (3)	1944 (2)	$(5^+,9^+)$	5^+	60 (7)
	773 (2)	$(5^+, 9^+)$	7^+	5 (1)
	455.6 (5)	$(5^+,9^+)$	$(5^+,7^+)$	6 (1)
4397 (3)	2698 (3)	$(5^+,9^+)$	5^+	11 (2)
	1288 (3)	$(5^+ ,9^+)$	(7^+)	23 (4)
	972 (2)	$(5^+ ,9^+)$	$(5^+ ,7^+)$	6 (2)
5293 (3)	2185 (3)		(7^+)	6 (2)
5829 (4)	1432 (3)		$(5^+ ,9^+)$	2.0 (5)
5999 (3)	2891 (3)		(7^+)	7 (2)
6136 (3)	3027 (3)		(7^+)	11 (3)
	2254 (3)			14 (3)
	1739 (4)			4 (1)
6944 (5)	3182 (4)		$(5^-,7^-)$	7 (2)
7468 (5)	1332 (4)			8 (2)
7858 (5)	3462 (4)		$(5^+,7^+)$	5 (2)

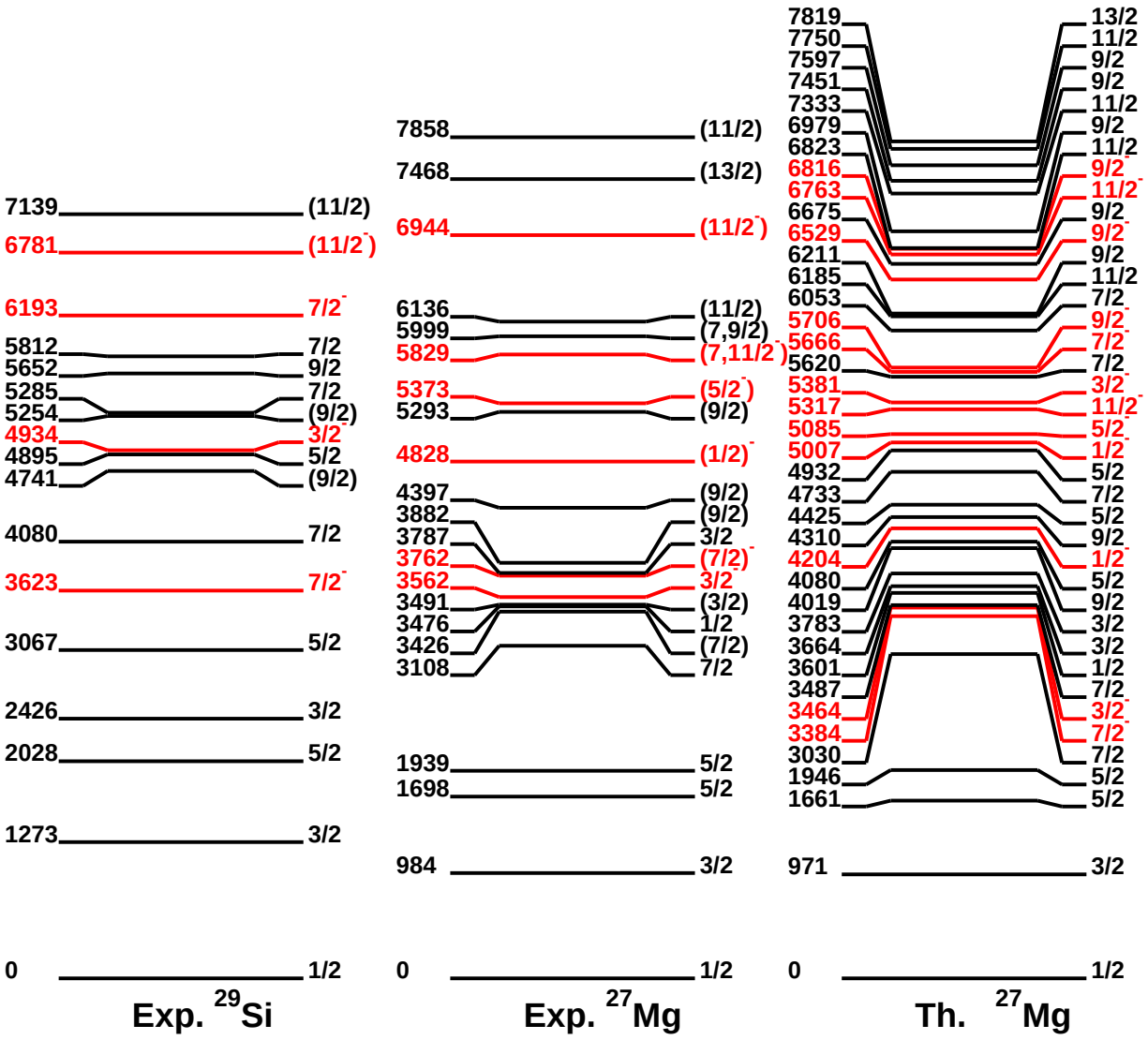

FIG. 11: A comparison of positive-parity excited states in ^{29}Si, ^{27}Mg, and shell model calculations for ^{27}Mg. Positive- (negative-) parity states are shown in black (red). The parities of states are positive unless indicated otherwise. Some previously reported states not observed in the present experiment are included for completeness. The theoretical calculations for positive-parity states use the shell model limited to the 1s-0d shell with the USDA interaction. Those for negative-parity states use the WBP-a interaction with one hole (particle) allowed in the 0p (0f-1p) shell. Only higher spin predicted states are shown at higher excitation energies.

TABLE III: Square-well estimates of neutron decay widths for higher spin unbound states in ^{27}Mg observed to γ decay in the present work and in Ref. [19]. The maximum parent state spins and, hence, neutron decay ℓ values are based on assuming M1 transitions.

$E_i(keV)$	J_i^π	$E_f(keV)$	$J_{f,max}^\pi$	l_{min}	$\Gamma_n(eV)$
6508	$(7/2^+)$	1939	$5/2^+$	4	2.8×10^{-4}
6651	$(9/2^+)$	3108	$7/2^+$	4	5.1×10^{-2}
6721	$(9/2^+)$	3426	$7/2^+$	4	1.7×10^{-1}
6811	$(9/2^+)$	3426	$7/2^+$	4	6.6×10^{-1}
6859	$(5/2^+)$	984	$3/2^+$	4	1.1×10^{0}
6921	$(9/2^-)$	3762	$7/2^-$	5	8.6×10^{-3}
6944 [a]	$(9/2^-)$	3762	$7/2^-$	5	1.1×10^{-2}
6991	$(7/2^+)$	1939	$5/2^+$	4	3.9×10^{0}
7013	$(5/2^+)$	984	$3/2^+$	2	$3.0 \times 10^{+4}$
7147	$(7/2^+)$	1939	$5/2^+$	4	$1.2 \times 10^{+1}$
7278	$(9/2^+)$	3426	$7/2^+$	4	$2.5 \times 10^{+1}$
7468 [a]	$(13/2^+)$	6136	$(11/2^+)$	6	3.1×10^{-3}
7505	$(7/2^+)$	1939	$5/2^+$	4	$7.3 \times 10^{+1}$
7530	$(9/2^-)$	3762	$7/2^-$	5	7.5×10^{-1}
7690	$(11/2^+)$	3882	$9/2^+$	6	1.1×10^{-2}
7700	$(7/2^+)$	1939	$5/2^+$	4	$1.5 \times 10^{+2}$
7858 [b]	$(11/2^+)$	4397	$9/2^+$	6	2.5×10^{-2}
7927	$(11/2^+)$	3882	$9/2^+$	6	3.4×10^{-2}
7976	$(7/2^+)$	1939	$5/2^+$	4	$3.6 \times 10^{+2}$

[a] Observed in the present experiment only.

[b] Observed in both the present experiment and in Ref. [19]

TABLE IV: Decay widths of low spin unbound states in ^{27}Mg measured in a neutron resonance experiment [31]. Also listed are the ratios of measured γ to neutron decay widths and measured neutron decay widths to calculated penetrabilities (spectroscopic factors S).

E_x (keV)	J^π	Γ_γ (eV)	Γ_N (eV)	Γ_γ/Γ_N	Penet. (eV)	S
6514	$1/2^-$	0.09	48	1.9×10^{-3}	1.9×10^{4}	2.5×10^{-3}
6671	$3/2^+$	1.1	80	1.4×10^{-2}	3.3×10^{3}	2.5×10^{-2}
6757	$1/2^-$	6.3	61200	1.0×10^{-4}	1.6×10^{5}	3.9×10^{-1}
6887	$1/2^+$	2.7	90	3.0×10^{-2}	3.3×10^{6}	2.7×10^{-5}
6898	$1/2^-$	3.4	11900	2.9×10^{-4}	2.5×10^{5}	4.7×10^{-2}
6963	$3/2^-$	0.5	260	1.9×10^{-3}	3.0×10^{5}	8.6×10^{-4}